BIOCHEMISTRY
including biophysical chemistry & molecular biology

ARTICLE

pubs.acs.org/biochemistry

Pleiotropic Impact of a Single Lysine Mutation on Biosynthesis of and Catalysis by *N*-Methyltryptophan Oxidase

Robert C. Bruckner, Jennifer Winans, and Marilyn Schuman Jorns*

Department of Biochemistry and Molecular Biology, Drexel University College of Medicine, Philadelphia, Pennsylvania 19102, United States

Supporting Information

ABSTRACT: *N*-Methyltryptophan oxidase (MTOX) contains covalently bound FAD. *N*-Methyltryptophan binds in a cavity above the *re* face of the flavin ring. Lys259 is located above the opposite, *si* face. Replacement of Lys259 with Gln, Ala, or Met blocks (>95%) covalent flavin incorporation in vivo. The mutant apoproteins can be reconstituted with FAD. Apparent turnover rates ($k_{cat,app}$) of the reconstituted enzymes are ~2500-fold slower than those of wild-type MTOX. Wild-type MTOX forms a charge-transfer E_{ox}·S complex with the redox-active anionic form of NMT. The E_{ox}·S complex formed with Lys259Gln does not exhibit a charge-transfer band and is converted to a reduced enzyme·imine complex (EH_2·P) at a rate 60-fold slower than that of wild-type MTOX. The mutant EH_2·P complex contains the imine zwitterion and exhibits a charge-transfer band, a feature not observed with the wild-type EH_2·P complex. Reaction of reduced Lys259Gln with oxygen is 2500-fold slower than that of reduced wild-type MTOX. The latter reaction is unaffected by the presence of bound product. Dissociation of the wild-type EH_2·P complex is 80-fold slower than k_{cat}. The mutant EH_2·P complex dissociates 15-fold faster than $k_{cat,app}$. Consequently, EH_2·P and free EH_2 are the species that react with oxygen during turnover of the wild-type and mutant enzyme, respectively. The results show that (i) Lys259 is the site of oxygen activation in MTOX and also plays a role in holoenzyme biosynthesis and *N*-methyltryptophan oxidation and (ii) MTOX contains separate active sites for *N*-methyltryptophan oxidation and oxygen reduction on opposite faces of the flavin ring.

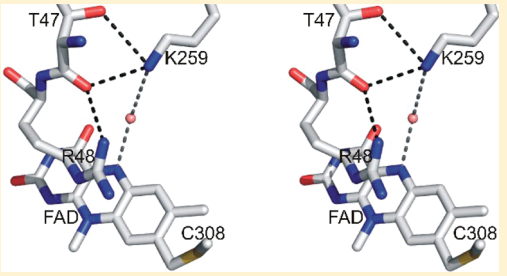

N-Methyltryptophan oxidase (MTOX) catalyzes the oxygen-dependent demethylation of *N*-methyl-L-tryptophan (NMT) to hydrogen peroxide and an unstable NMT imine that is hydrolyzed to produce L-tryptophan and formaldehyde. Other *N*-methyl amino acids, such as sarcosine, and carbinolamines are poor alternate substrates. Steady-state kinetic studies indicate that NMT oxidation occurs via a ternary complex mechanism in which oxygen reacts with a reduced enzyme·NMT imine complex.[2]

MTOX is expressed as a constitutive enzyme in *Escherichia coli*. Expression is enhanced in minimal medium but not induced by NMT. MTOX is a monomeric flavoprotein.[3] The flavin cofactor [8α-(*S*-cysteinyl)FAD] is covalently bound to the protein via a thioether linkage to Cys308.[4,5] MTOX is a member of a family of prokaryotic and eukaryotic amino acid oxidases that contain covalently bound flavin.[6−9] MTOX exhibits the highest degree of sequence homology (43% identical) with monomeric sarcosine oxidase (MSOX), a bacterial enzyme whose expression is induced by sarcosine, a common soil metabolite.[10] NMT is not a substrate for MSOX.

The crystal structure of MTOX has been determined at 3.2 Å resolution.[5] MTOX is a two-domain protein. FAD is bound in an extended configuration. The flavin ring is located at the interface between the flavin and catalytic domains. A model of a MTOX·NMT complex shows that the substrate is readily accommodated in a cavity above the *re* face of the flavin ring. The architecture of the NMT-binding cavity is similar to that observed for the sarcosine-binding cavity in MSOX with the notable substitution of residues lining the entrance of the cavity that appear to be important determinants of the different substrate specificities of the enzymes.

The principles that govern the oxygen reactivity of flavoxidases are poorly defined and a subject of considerable current interest. Reduction of oxygen to hydrogen peroxide by free reduced flavin is thermodynamically favorable but kinetically slow because the two-electron reduction of triplet oxygen by a diamagnetic organic molecule is spin-forbidden.[11,12] Instead, the reaction proceeds via an initial one-electron-transfer step that generates a flavin radical/superoxide anion radical pair in a spin-allowed but energetically unfavorable, rate-determining reaction (Scheme 1). The accelerated rate of oxygen reduction observed with oxidases is called oxygen activation.

Recent studies with MSOX show that (i) oxygen reduction occurs on the opposite side of the flavin ring (*si* face) compared with the sarcosine-binding cavity and (ii) mutation of Lys265 to a neutral residue results in an ~10000-fold decrease in the reaction

Received: March 9, 2011
Revised: April 8, 2011
Published: April 28, 2011

rate.[13,14] Lys259 in MTOX is located above the *si* face of the flavin ring, similar to that observed for Lys265 in MSOX. The lower-resolution MTOX structure does not contain water molecules. A water molecule has been modeled into the putative *si* face active site in MTOX on the basis of an alignment with MSOX. The model suggests that Lys259 is hydrogen bonded to FAD N5 via a bridging water molecule (Figure 1). A conserved lysine is found above the *si* face of the flavin ring in nearly all members of the MTOX−MSOX family of amino acid oxidases with the notable exception of nikD. In fact, the reaction of free reduced nikD with oxygen is very slow, similar to the corresponding reaction with free flavin. However, an accelerated rate of oxygen reduction is observed with reduced nikD·ligand complexes.[15]

The results suggest that Lys259 may play a role in oxygen activation by MTOX. However, a very different scenario is also possible, as judged by results obtained for a highly conserved histidine residue in members of the glucose-methanol-choline oxidase family. Mutagenesis studies show that the histidine is solely responsible for oxygen activation by glucose oxidase. In contrast, a different function is observed for the corresponding histidine in choline oxidase where oxygen activation is mediated by the positively charged headgroup in choline oxidation products.[16,17]

In this paper, we show that Lys259 is the site of oxygen activation in MTOX. Replacement of Lys259 with a neutral residue also reveals an impressive range of other functions, as judged by the multiple effects of the mutation on holoenzyme biosynthesis and amino acid oxidation.

Scheme 1. Postulated Mechanism for the Reduction of Oxygen by Reduced Flavin[a]

[a] In a variant of this mechanism, the radical pair is converted to the same products via the intermediate formation of a 4a-peroxy flavin (not shown). This intermediate is commonly observed with monooxygenases but only rarely with oxidases. Abbreviation: rds, rate-determining step.

EXPERIMENTAL PROCEDURES

Materials. Restriction enzymes and T4 DNA ligase were obtained from New England Biolabs. Horseradish peroxidase, *o*-dianisidine, and *N*-methyl-L-tryptophan were purchased from Sigma. Amplex Red was obtained from Molecular Probes.

Subcloning the Gene for Wild-Type MTOX To Append a C-Terminal His_6 Tag. Plasmid pESOX1 contains the cloned gene for MTOX from *E. coli*.[4] Polymerase chain reaction (PCR) was used to introduce an *Nde*I restriction site at the 5′ end of the gene, delete the stop codon, and introduce an *Xho*I restriction site at the 3′ end of the gene. The PCR was performed using pESOX1 as a template, Taq polymerase (Qiagen), 5′-CATATGAAATACGATCTCATCATTATTGG-3′ (forward primer), and 5′-CTCGAGTTGGAAGCGGGAAAGCCTGAATGG-3′ (reverse primer). The PCR product was purified and ligated with TA cloning vector pCR2.1 (Invitrogen). The resulting plasmid was transferred into *E. coli* INVαF′ (Invitrogen). Transformants were subjected to blue-white screening. Plasmid DNA was isolated from a white colony and digested with *Nde*I and *Xho*I. The fragment containing the MTOX gene was subcloned between the *Nde*I and *Xho*I sites of plasmid pET23a (Novagen) to yield plasmid pWZ01. Plasmid pWZ01 was used to transform *E. coli* BL21(DE3) cells to ampicillin resistance. A clone containing the desired plasmid was sequenced in both directions across the entire sequence of the MTOX gene. Sequencing was conducted by MWG/Operon.

Mutation of Lys259 to Gln, Ala, or Met. Mutations were generated by using plasmid pWZ01 as a template, *Pfu* DNA polymerase (Stratagene), and the overlap extension PCR method described by Ho et al.[18] The left-hand fragment was generated using START (external primer) as the forward primer and an internal backward primer containing the desired mutation (data not shown; see Table S1 of the Supporting Information). The right-hand fragment was generated using an internal forward primer containing the desired mutation and END (external primer) as the backward primer. The purified left- and right-hand fragments were combined using START and END as forward and backward primers, respectively. The final PCR product was purified, digested with *Nde*I and *Xho*I, purified

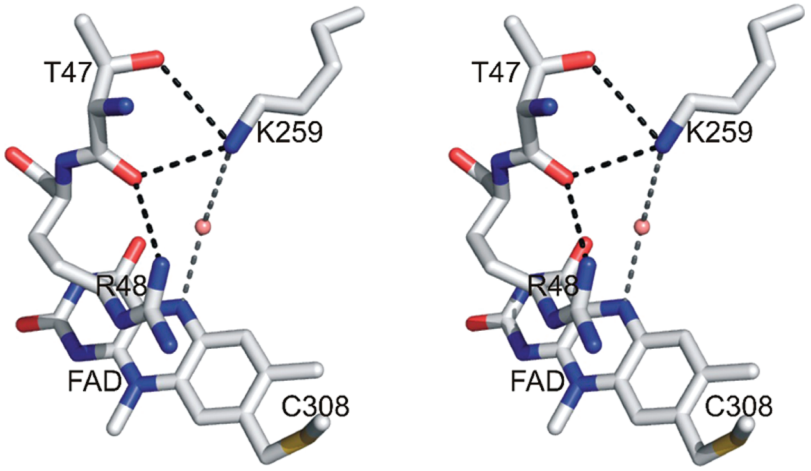

Figure 1. Stereoview of the region above the *si* face of the flavin ring in wild-type MTOX (PDB entry 2UZZ). Carbon atoms are colored white, nitrogen atoms blue, and oxygen atoms red. Hydrogen bonds are represented as dashed black lines. The MTOX PDB file does not contain any waters. A water molecule (light red sphere) and putative hydrogen bonds (dashed gray lines) have been modeled into the MTOX active site on the basis of an alignment with monomeric sarcosine oxidase (PDB entry 2GBO), as described in the text. The diagram was rendered using PYMOL (http://www.pymol.org).

again, and then subcloned between the *Nde*I and *Xho*I sites of plasmid pET23a. The resulting construct was used to transform *E. coli* BL21(DE3) cells to ampicillin resistance. Plasmids that exhibited the expected insert size (p3:K259Q, p1:K259A, and p2:K259N for the Lys259Gln, Lys259Ala, and Lys259Met mutations, respectively) were isolated and sequenced in both directions across the entire insert. Sequencing was conducted by MWG/Operon.

Expression and Purification of Wild-Type MTOX. *E. coli* BL21(DE3)/pWZ01 cells were grown at 37 °C in Terrific Broth containing ampicillin (100 μg/mL) until the A_{595} reached 0.9. MTOX expression was induced with isopropyl β-D-thiogalactopyranoside (IPTG) (0.5 mM). Cells were harvested after an overnight incubation. All steps of the purification were conducted at 4 °C. Cells were disrupted by sonication in the presence of protease inhibitors, as previously described.[4] The supernatant obtained after centrifugation was incubated with 25 mL of Ni-NTA agarose (Qiagen) for 1 h at 4 °C and then poured into a column containing a 10 mL bed of Ni-NTA agarose. The column was washed with 50 mM potassium phosphate buffer (pH 8.0) containing 500 mM NaCl, 15 mM imidazole, and 10% (w/v) glycerol. MTOX was eluted using a 1 L linear gradient from 15 to 500 mM imidazole. Pooled fractions were dialyzed versus 50 mM potassium phosphate (pH 8), concentrated, and stored in aliquots at −80 °C.

Expression and Purification of Lys259 Mutants. A similar procedure was used for expression and purification of the mutant enzymes except that cells were grown at 18 °C and harvested ~30 h after induction with IPTG.

Reconstitution of Lys259 Mutants with FAD. The isolated mutant enzymes were incubated for 12 h at room temperature in Tris (35 mM)/potassium phosphate (10 mM) buffer (pH 8.0) containing 0.5 mM FAD. Unbound flavin was removed by ultrafiltration, and the buffer was changed to 50 mM potassium phosphate (pH 8) using a CentriPrep YM30 membrane. The concentrated reconstituted preparations were stored in aliquots at −80 °C.

Characterization of the Chromophore(s) in Lys259 Mutants. Absorption spectra were recorded using an Agilent Technologies 8453 diode array spectrophotometer. Samples of the isolated and FAD-reconstituted enzymes were denatured with 3 M guanidine hydrochloride and then subjected to ultrafiltration using a Microcon 10 concentrator to determine whether the chromophores in the preparations were covalently attached to the proteins. Extinction coefficients of oxidized FAD at 450 nm and the stoichiometry of FAD incorporation were determined after denaturation of the FAD-reconstituted enzymes with guanidine hydrochloride, as previously described.[4] Extinction coefficients of reduced FAD at 450 and 427 nm were determined after anaerobic reduction of reconstituted Lys259Gln with 2.0 mM NMT (ε_{450} = 2740 M^{-1} cm^{-1}; ε_{427} = 3340 M^{-1} cm^{-1}). The amount of FAD in the isolated mutant preparations was estimated on the basis of the amount of flavin that can be reduced by substrate (2 mM NMT). The absorbance of the substrate-reduced preparations at 427 nm was corrected for the contribution due to reduced FAD and used to estimate the 6-hydroxyFAD content (ε_{427} = 22600 M^{-1} cm^{-1}).[19]

Activity and Protein Assays. Wild-type MTOX activity was measured using a horseradish peroxidase-coupled assay with *o*-dianisidine as the chromogenic substrate (ε_{460} = 6770 M^{-1} cm^{-1}), as previously described.[4] However, a more sensitive assay was required to monitor activity with the Lys259 mutants. This was achieved by replacing *o*-dianisidine with Amplex Red (ΔA_{563} = 52200 M^{-1} cm^{-1}).[20] Protein was determined as previously described.[4] The enzyme concentration was also determined on the basis of the absorbance of covalently bound FAD using a previously determined extinction coefficient for wild-type MTOX (ε_{457} = 13300 M^{-1} cm^{-1})[4] and values determined in this study for Lys259Gln, Lys259Ala, and Lys259Met (ε_{450} = 13100, 13100, and 13800 M^{-1} cm^{-1}, respectively).

Kinetics of the Anaerobic Reaction of Wild-Type MTOX or Lys259Gln with *N*-Methyl-L-tryptophan. Rapid reaction kinetic measurements were performed by using a Hi-Tech Scientific SF-61DX2 stopped-flow spectrometer (dead time of 1.7 ms) in diode array mode. Data were collected in log mode to maximize the number of points acquired during the early phase of each reaction. All spectra are the averages of at least three replicate shots. Reactions were conducted at 25 °C in 100 mM potassium phosphate buffer (pH 8.0) containing 50 mM glucose and glucose oxidase (14.7 units/mL). Tonometers containing enzyme or substrate and the entire flow circuit of the stopped-flow spectrometer were made anaerobic by multiple cycles of evacuation and flushing with oxygen-scrubbed argon in conjunction with a glucose/glucose oxidase system, as previously described.[21] The integration time for each spectrum is 1.5 ms; the indicated time for each spectrum is that after data collection had been triggered.

Kinetics of the Reaction of Reduced Lys259Gln with Oxygen. A concentrated stock solution of reduced Lys259Gln in 100 mM potassium phosphate buffer (pH 8.0) at 25 °C was prepared by reaction with 1 equiv of NMT in an anaerobic cuvette. A 50 μL aliquot of the reduced enzyme was anaerobically transferred into a screw-cap cuvette equipped with a Teflon−silicon membrane (Spectrocell) using a gastight Hamiliton syringe, as previously described.[13] The screw-cap cuvette contained 450 μL of 100 mM potassium phosphate buffer (pH 8.0) at 25 °C that had been equilibrated with water-saturated oxygen/nitrogen gas mixtures. The reactions were monitored using an Agilent Technologies model 8453 diode array spectrophotometer.

Kinetics of the Reaction of Reduced Wild-Type MTOX with Oxygen. A solution of reduced wild-type enzyme was prepared in a stopped-flow tonometer. The main compartment was filled with 100 mM potassium phosphate buffer (pH 8.0) containing 1 equiv of NMT. A concentrated aliquot of enzyme was placed in a side arm. The solutions were made anaerobic as described above, except the glucose/glucose oxidase system was omitted. Traces of residual oxygen were removed by bubbling oxygen-scrubbed argon gas through the buffer in the main compartment and over the surface of the enzyme in the side arm. The enzyme was then tipped into the main compartment of the tonometer and incubated for 30 min at room temperature to ensure complete reduction. Solutions containing reduced enzyme were mixed (1:1) in the stopped-flow spectrometer with 100 mM potassium phosphate buffer (pH 8.0) that had been equilibrated with water-saturated oxygen/nitrogen gas mixtures.

Data Analysis. Global analysis of stopped-flow diode array data sets was performed using Specfit 3.0. Fitting of single-wavelength kinetic traces was conducted by using Kinetic Studio 2.14a (TgK Scientific). All other data analyses were performed using Sigma Plot 10 (Systat Software). Spectra corresponding to 100% complex formation were calculated by using observed dissociation constants and spectra recorded for the free enzyme and at the highest ligand concentration tested, as previously described.[22]

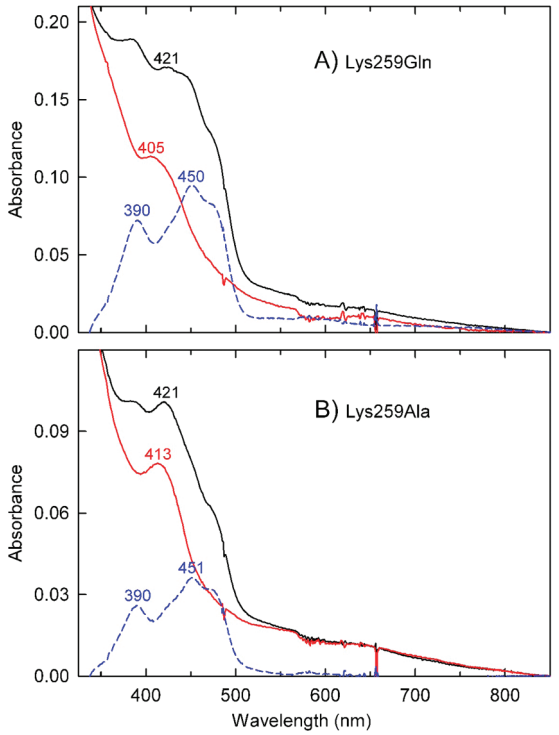

Figure 2. Spectral properties of the isolated preparations of Lys259Gln and Lys259Ala. Spectra were recorded in 50 mM potassium phosphate buffer (pH 8.0) at 25 °C. The solid black and red curves in each panel were obtained before and immediately after addition of 1.6 mM NMT, respectively. The dashed blue curves are difference spectra, calculated via subtraction of the spectrum of the substrate-reduced enzyme from the corresponding spectrum of the untreated enzyme.

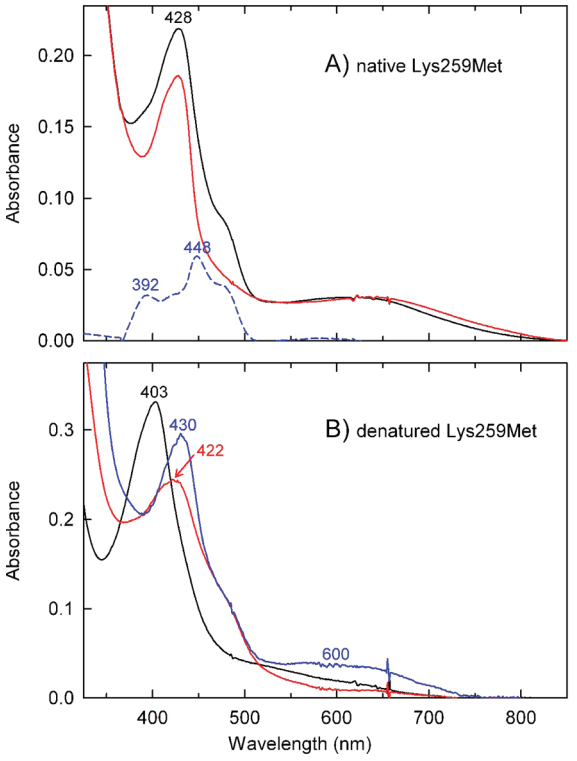

Figure 3. Spectral properties of Lys259Met. (A) The solid black and red curves were recorded before and immediately after addition of 2.0 mM NMT, respectively, in 50 mM potassium phosphate buffer (pH 8.0) at 25 °C. The dashed blue curve is the difference spectrum, calculated as described in the legend of Figure 2. (B) Absorption spectra of denatured Lys259Met were recorded in 100 mM Tris-HCl (pH 9.0) (blue), 100 mM sodium acetate (pH 5.0) (red), or 6 N HCl (black) containing 3 M guanidine hydrochloride at 25 °C.

RESULTS

Effect of Lys259 Mutations on the Expression of the MTOX Holoenzyme. A His_6 tag is appended to the C-terminus of MTOX to facilitate the purification of wild-type and mutant enzymes. Pure His_6-tagged wild-type enzyme is isolated using a single metal affinity chromatography step. The preparation contains covalently bound FAD and exhibits spectral and catalytic properties virtually identical to those reported for the untagged enzyme (data not shown; see Table S2 of the Supporting Information), purified using salt fractionation and several chromatography steps.[4] The results show that the introduction of a His_6 tag does not affect the expression of the MTOX holoenzyme.

Mutation of Lys259 to a neutral residue (Gln, Ala, or Met) results in the isolation of apparently pure preparations that do not, however, exhibit a typical flavoprotein absorption spectrum. Somewhat different spectral properties are observed for each mutant, but all exhibit significant absorption in the long-wavelength region ($\lambda > 600$ nm) and a maximum in the 421−428 nm region (black curves in Figures 2 and 3A). Each mutant preparation was denatured with 3 M guanidine hydrochloride and subjected to ultrafiltration using a Microcon 10 concentrator. In each case, protein and chromophore absorbance are found only in the retentate (data not shown). The results indicate that the chromophores in the mutant preparations are covalently attached to the protein.

Covalently bound FAD in wild-type MTOX is immediately reduced upon manual mixing with excess *N*-methyl-L-tryptophan (NMT) (2 mM) under aerobic conditions. A similar experiment with the mutant enzymes results in a partial loss of absorption above 300 nm (red curves in Figures 2 and 3A). Spectra observed for the NMT-reduced enzymes were subtracted from spectra obtained for the corresponding oxidized preparations. The resulting difference spectra exhibit peaks around 450 and 390 nm, typical of that expected for a flavoprotein (blue curves in Figures 2 and 3A). The data show that the mutant preparations contain covalently bound FAD. However, the preparations exhibit values for the A_{280}/A_{450} ratio that are 20−40-fold higher than that observed with wild-type MTOX (Table 1), which contains a nearly stoichiometric amount of FAD. The results indicate that the mutant enzyme preparations contain only a small amount of FAD. Furthermore, the atypical spectral properties strongly suggest that the mutant preparations also contain a second chromophore.

Characterization of the Second Chromophore in Lys259Met. The spectral properties of Lys259Met, especially the value obtained for the A_{420}/A_{450} ratio (Table 1), suggested that the second chromophore is the predominant species in this mutant. Unlike substrate reduction, both chromophores in Lys259Met are readily and reversibly reduced with dithionite (data not shown), indicating that the second chromophore contains an oxidation−reduction system.

The absorption spectrum of Lys259Met is strikingly similar to that observed for free 6-hydroxyFAD when the phenolic hydroxyl group is deprotonated ($pK_a = 7.1$) (Scheme 2).[19] Noncovalently

Table 1. Comparison of the Spectral and Catalytic Properties of Lys259 Mutants with Those of Wild-Type MTOX[a]

	untreated			reconstituted		activity[d]
preparation	A_{420}/A_{45X}	A_{280}/A_{45X}	mol of FAD/mol of 6-OH FAD[b]	A_{280}/A_{45X}	mol of FAD/mol of protein[c]	$k_{cat,app}$ (s^{-1})
wild-type	0.62	7.13	–	–	0.90	21.4 ± 0.6
Lys259Gln	1.07	212	3.00	18.3	0.36	0.0166 ± 0.0007
Lys259Ala	1.30	267	1.30	20.3	0.32	0.0083 ± 0.0002
Lys259Met	1.58	134	0.73	23.2	0.26	0.0021 ± 0.0001

[a] A_{45X} is A_{450} (Lys259 mutants) or A_{457} (wild-type MTOX). [b] The molar ratio of the two flavins was determined as described in Experimental Procedures using the data shown in Figures 2 and 3A. [c] The covalent FAD content of untreated wild-type MTOX or reconstituted mutant enzymes was determined as described in Experimental Procedures. [d] The activity of the untreated wild-type enzyme or reconstituted mutant enzymes was measured using a horseradish peroxidase-coupled assay with Amplex Red as the chromogenic substrate. The enzyme concentration was estimated on the basis of flavin absorbance, as described in Experimental Procedures.

Scheme 2. Structure and Ionization of 6-HydroxyFAD

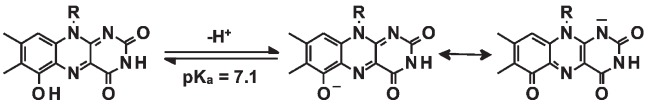

Table 2. Characterization of the Second Chromophore in Lys265Met

	denatured Lys265Met		free 6-hydroxyFAD[a]	
	λ_{max}	ε at λ_{max} (relative)[b]	λ_{max}	ε at λ_{max} (relative)[b]
6 N HCl	403	1.00	403	1.00
pH 5.0	422	0.74	422	0.63
pH 9.0	430	0.89	427	0.73
	600	0.11	600	0.11

[a] The spectral properties of free 6-hydroxyFAD were previously reported.[19] [b] Extinction coefficients are expressed relative to that observed in 6 N HCl. The extinction coefficient of free 6-hydroxyFAD in 6 N HCl is 31000 M^{-1} cm^{-1}.[19]

bound 6-hydroxyFAD is found in at least seven flavoenzymes.[19,23−27] Free 6-hydroxyFAD exhibits characteristic spectral changes as a function of pH.[19] The effect of pH on the spectral properties of Lys259Met was determined after the enzyme had been denatured with 3 M guanidine hydrochloride to minimize interference because of the protein moiety (Figure 3B). Denatured Lys259Met at pH 9.0 exhibits absorption maxima at 430 and 600 nm. The long-wavelength absorption band is eliminated when the pH is decreased to 5.0, accompanied by a hypsochromic shift of the 430 nm band to 422 nm. A much larger hypsochromic shift to 403 nm is observed in 6 N HCl. Very similar pH-dependent spectral changes are observed with free 6-hydroxyFAD and are attributed to protonation of the 6-phenolate substituent and the N1 position in the flavin ring ($pK_a \sim 0$) (Table 2).

Reconstitution of the Lys259 Mutant Preparations with FAD. The results show that the Lys259 mutant preparations contain covalently bound FAD and 6-hydroxyFAD. The relative amount of FAD and 6-hydroxyFAD is apparently sensitive to the nature of the amino acid substitution, as judged by values obtained for the ratio of the two flavins (see Table 1). However, all three mutants exhibit very high values for the ratio of absorbance at 280 nm to that in the visible region (see Table 1) and, therefore, must contain predominantly apoprotein. Previous studies with MSOX show that covalent flavin attachment occurs in an autocatalytic reaction upon mixing the isolated wild-type apoprotein with FAD.[20] Indeed, reconstitution of the MTOX mutant preparations is observed after incubation with FAD, as judged by the dramatic decrease in the A_{280}/A_{450} ratio (see Table 1). The flavin is bound covalently, as judged by results obtained upon ultrafiltration after denaturation of the reconstituted preparations.

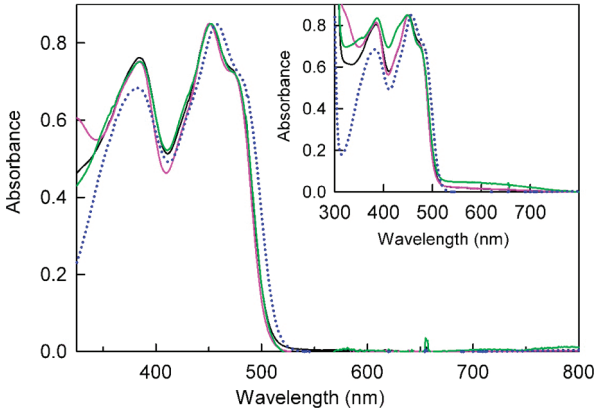

Figure 4. Reconstitution of the isolated Lys259 mutant preparations with FAD. Spectra were recorded in 50 mM potassium phosphate buffer (pH 8.0) at 25 °C. The solid black, magenta, and green curves are difference spectra obtained for reconstitution of Lys259Gln, Lys259Ala, and Lys259Met, respectively. The spectra were calculated via subtraction of spectra observed before from those observed after reconstitution with FAD and are normalized to the same absorbance at 450 nm. The solid black, magenta, and green curves shown in the inset are the corresponding absolute absorption spectra of the reconstituted enzymes, also normalized to the same absorbance at 450 nm. For comparison, the absorption spectrum of wild-type MTOX is shown as the dotted blue curve in the main panel and the inset.

The spectral properties of the flavin incorporated during in vitro reconstitution were determined by subtraction of absorption spectra observed for the initial preparations from those observed for the corresponding reconstituted preparations. Nearly identical difference spectra were obtained for all three mutants (Figure 4). The calculated difference spectra exhibit maxima around 450 and 385 nm, similar to that expected for a typical flavoprotein The results indicate that in vitro reconstitution results in the exclusive incorporation of unmodified FAD.

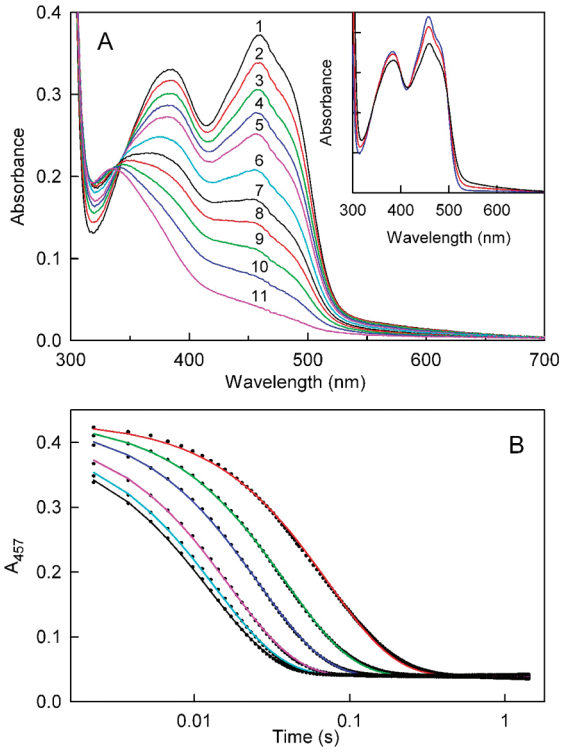

Figure 5. Fast phase of the anaerobic reaction of wild-type MTOX with NMT. Reactions were monitored by stopped-flow diode array spectroscopy. (A) Curves 1 to 11 were recorded 0.74, 2.24, 3.74, 5.24, 6.74, 9.74, 12.7, 15.7, 20.2, 27.7, and 64.5 ms, respectively, after 33.1 μM enzyme had been mixed with 2000 μM NMT in 100 mM potassium phosphate buffer (pH 8.0) at 25 °C. In the inset, the blue, red, and black curves were recorded 0.74 ms after MTOX had been mixed with 0, 500, and 2000 μM NMT, respectively. (B) The red, green, blue, magenta, cyan, and black curves were obtained by fitting a monoexponential equation ($y = Ae^{-k_{fast}t} + B$) to data (●) recorded at 457 nm after MTOX had been mixed with 150, 300, 500, 1000, 1500, and 2000 μM NMT, respectively.

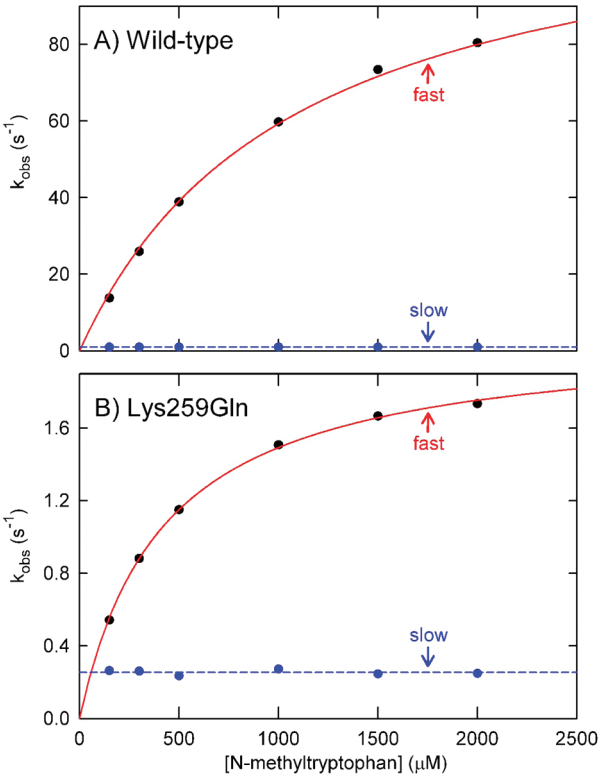

Figure 6. Effect of NMT concentration on the observed rate of the fast and slow phases of the anaerobic half-reactions observed with wild-type MTOX (A) or Lys259Gln (B). Values for k_{fast} and k_{slow} with wild-type MTOX were obtained by analysis of spectral changes at 457 and 355 nm, respectively. Values for k_{fast} and k_{slow} with Lys259Gln were obtained by analysis of the biphasic absorbance change at 457 nm; similar values were obtained by global analysis of the data (see Table 3). In each panel, the red lines were obtained by fitting a hyperbolic equation [$k_{obs} = (k_{lim}[NMT])/(K_{d,app} + [NMT])$] to the values obtained for k_{fast} (●); the dashed blue lines correspond to the average value obtained for k_{slow} (blue circles).

The reconstituted mutant preparations contain ~30−40% of the FAD content of wild-type MTOX (see Table 1). Similar absolute spectra are observed for reconstituted Lys259Gln and Lys259Ala, except for a modest difference in the near-UV region that can be attributed to a larger amount of residual apoprotein in the latter preparation (Figure 4, inset). In comparison, the absolute absorption spectrum of reconstituted Lys259Met exhibits higher absorbance in the 420 nm region (Figure 4, inset) because of the higher 6-hydroxyFAD content in this preparation.

Turnover of the reconstituted mutant preparations with 1 mM NMT in air-saturated buffer could be detected using a sensitive horseradish peroxidase-coupled assay with Amplex Red as the chromogenic substrate. The apparent k_{cat} observed with wild-type MTOX under these conditions ($k_{cat,app} = 21.4 \pm 0.6\ s^{-1}$) is ~30% of the maximal turnover rate observed at saturating concentrations of NMT and oxygen ($k_{cat} = 77 \pm 15\ s^{-1}$).[2] Mutation of Lys259 to Gln, Ala, or Met results in a 1300-, 2500-, or 10000-fold decrease, respectively, in turnover rate, as judged by the values obtained for $k_{cat,app}$ (Table 1). The results show that replacing Lys259 with a neutral residue has a profound effect on catalytic activity. As described in the following sections, reductive and oxidation half-reaction studies with wild-type MTOX and Lys259Gln were conducted to assess the impact of the Lys259 mutation on the rate of NMT oxidation and oxygen reduction, respectively.

Fast Phase of the Anaerobic Reaction of Wild-Type MTOX with NMT. An isosbestic loss of oxidized flavin absorbance is observed when the reductive half-reaction with wild-type MTOX is monitored using a stopped-flow spectrometer in diode array mode (Figure 5A). The decrease in absorbance at 457 nm exhibits apparent first-order kinetics, as judged by the single-exponential fits obtained at all substrate concentrations tested (Figure 5B). The observed apparent first-order rate constants (k_{obs}) exhibit a hyperbolic dependence on NMT concentration (Figure 6A). Values for the limiting rate of enzyme reduction at saturating NMT and the apparent dissociation constant of the enzyme·substrate complex were estimated by fitting the data to

$$k_{obs} = (k_{lim}[NMT])/(K_{d,app} + [NMT]) \quad (1)$$

The results for the fast phase are consistent with the mechanism shown in the first two steps of Scheme 3, in which formation of an oxidized enzyme·substrate complex (E_{ox}·NMT) is followed by an effectively irreversible flavin reduction step (k_{lim}) that produces a reduced enzyme·imine product complex (EH_2·P). The value obtained for k_{lim} ($129 \pm 3\ s^{-1}$) is 1.7-fold larger than a value obtained for k_{cat} in previous steady-state kinetic studies

dx.doi.org/10.1021/bi200349m |*Biochemistry* 2011, 50, 4949–4962

($77 \pm 15\ s^{-1}$).[2] The results indicate that the fast phase is kinetically competent and that substrate oxidation may be partly rate-determining during aerobic turnover. The apparent second-order rate constant for the reaction of MTOX with NMT, as estimated from stopped-flow data [$k_{lim}/K_{d,app} = (1.10 \pm 0.06) \times 10^5\ M^{-1}\ s^{-1}$], is in good agreement with a value calculated using steady-state kinetic parameters [$k_{cat}/K_{m,NMT} = (2.0 \pm 0.6) \times 10^5\ M^{-1}\ s^{-1}$] (Table 3).

For the mechanism shown Scheme 3, $K_{d,app}$ is equal to $(k_{-1} + k_{lim})/k_1$. Thus, in the case of a sticky substrate ($k_{-1} \ll k_{lim}$), $K_{d,app}$ is not equivalent to the K_d for the $E_{ox}\cdot S$ complex ($K_d = k_{-1}/k_1$). On the other hand, similar values are expected for $K_{d,app}$ and K_d in the case of a nonsticky substrate ($k_{-1} \gg k_{lim}$). To distinguish between these scenarios, we sought to measure the K_d for the $E_{ox}\cdot S$ complex. Initial spectra recorded after MTOX had been mixed with different concentrations of NMT differ from that observed for the substrate-free oxidized enzyme, especially with regard to the development of absorbance in the long-wavelength region ($\lambda > 550$ nm) (Figure 5A, inset), a feature diagnostic of charge-transfer interaction. The results indicate

Scheme 3. Proposed Mechanism for the Anaerobic Reaction of Wild-Type MTOX with *N*-Methyl-L-tryptophan (NMT) (P = NMT imine)[a]

$$E_{ox} \underset{k_{-1}}{\overset{k_1[NMT]}{\rightleftharpoons}} E_{ox}\bullet NMT \quad (1)$$

$$E_{ox}\bullet NMT \underset{k_r}{\overset{k_{lim}}{\rightleftharpoons}} EH_2\bullet P \quad (2)$$

$$EH_2\bullet P \xrightarrow{k_{slow}} EH_2 + P \quad (3)$$

$$EH_2 \underset{k_{-3}}{\overset{k_3[NMT]}{\rightleftharpoons}} EH_2\bullet NMT \quad (4)$$

[a] The oxidation of NMT (step 2) is shown as a reversible reaction, as required on the basis of the intersecting line double-reciprocal plots obtained in steady-state kinetics studies.[2] However, the observed hyperbolic dependence of k_{obs} on the concentration of NMT (see eq 1) indicates that k_r has a negligible value. Furthermore, values for k_r that are not significantly different from zero are obtained upon fitting a three-parameter hyperbolic equation [$k_{obs} = k_r + (k_{lim}[NMT])/(K_{d,app} + [NMT])$] to the data. Only steps 1 and 2 occur during aerobic turnover of wild-type MTOX, as discussed in the text.

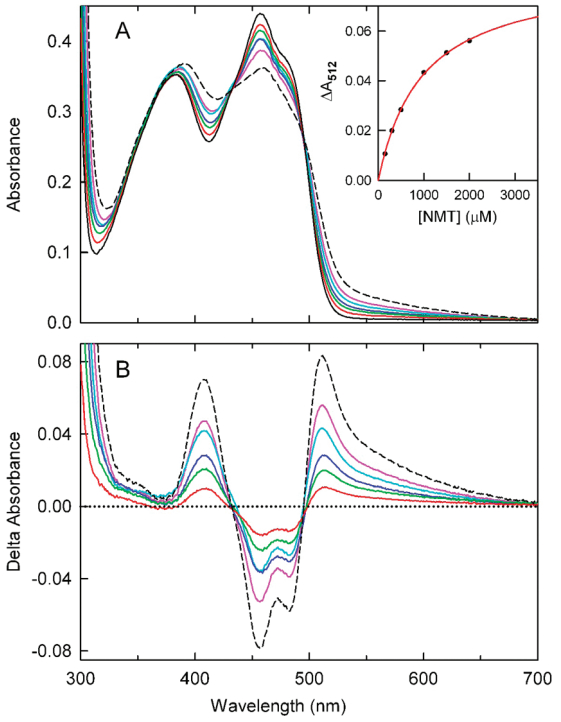

Figure 7. Calculated absorption spectra for the charge-transfer enzyme·substrate complex formed upon mixing wild-type MTOX with NMT. Spectra were calculated by global analysis of diode array stopped-flow data at various concentrations of NMT, as described in the text. The solid black curve in panel A is the spectrum of free MTOX. Calculated spectra for the mixture of free E and the ES complex formed with 150, 300, 500, 1000, and 2000 μM NMT are shown by the solid red, green, blue, cyan, and magenta curves, respectively. The dashed black curve shows the spectrum calculated for 100% complex formation, as described in Experimental Procedures. The corresponding difference spectra, obtained by subtracting the spectrum of free MTOX from spectra calculated at various NMT concentrations, are shown in panel B. The inset in panel A shows a plot of the absorbance increase at 512 nm vs the NMT concentration. The solid red line is a fit of a theoretical binding curve [$\Delta A_{obs} = (\Delta A_{max}[ligand])/(K_d + [ligand])$] to the data (●).

Table 3. Kinetic Parameters for the Reductive Half-Reaction of Wild-Type MTOX or the Lys259Gln Mutant with *N*-Methyl-L-tryptophan

		reductive half-reaction							
						spectral K_d (μM)[c]		steady-state turnover[a]	
preparation	phase	λ (nm)[b]	k_{lim} (s^{-1})	$K_{d,app}$ (μM)	$k_{lim}/K_{d,app}$ ($M^{-1}\ s^{-1}$)	$E_{ox}\cdot NMT$	$EH_2\cdot NMT$	k_{cat} (s^{-1})	$k_{cat}/K_{m\ NMT}$ ($M^{-1}\ s^{-1}$)
wild-type	k_{fast}	457	129 ± 3	1168 ± 59	$(1.10 \pm 0.06) \times 10^5$	973 ± 42	934 ± 218	77 ± 15	$(2.0 \pm 0.6) \times 10^5$
	k_{slow}[d]	355	0.981 ± 0.004						
Lys259Gln	k_{fast}	457	2.13 ± 0.02	424 ± 13	$(5.02 \pm 0.16) \times 10^3$	569 ± 39			
		global	2.12 ± 0.02	368 ± 14	$(5.61 \pm 0.21) \times 10^3$				
	k_{slow}[d]	457	0.244 ± 0.007						
		355	0.255 ± 0.006						
		global	0.276 ± 0.003						

[a] Data previously reported.[2] [b] Absorbance changes at the indicated wavelength were used in analyzing the kinetics of the specified phase of the reductive half-reaction. Global analysis of spectral changes was conducted using Specfit, as described in the text. [c] Spectral K_d values were determined as described in the legends of Figures 7–9. [d] The observed rate of the slow phase is independent of the concentration of NMT. The reported value is the average of values obtained with various concentrations of NMT in the range from 150 to 2000 μM.

dx.doi.org/10.1021/bi200349m |*Biochemistry* 2011, 50, 4949–4962

that an E_{ox}·S charge-transfer complex is formed within the instrument dead time. However, partial conversion of E_{ox}·S to EH_2·P also occurs during mixing, particularly at higher substrate concentrations. To obtain a calculated spectrum for the E_{ox}·S complex, we globally analyzed the fast phase of the reaction ($5t_{1/2}$) at each NMT concentration tested by fitting the data to an A ⟹ B ⟹ C model. In this model, A is free E_{ox}, B is an equilibrium mixture of E_{ox} and E_{ox}·S, and C is EH_2·P. Calculated spectra for B at different substrate concentrations are nearly isosbestic and exhibit progressive formation of a charge-transfer absorption band as the substrate concentration is increased (Figure 7A). The charge-transfer band exhibits a maximum at 512 nm, as judged by the position of the peak observed in the corresponding difference spectra (Figure 7B). A dissociation constant for the complex was estimated by fitting a theoretical binding curve to the observed absorbance increases at 512 nm (Figure 7A, inset). The value obtained for the dissociation constant of the E_{ox}·S complex (K_d = 973 ± 42 μM) is very similar to the value obtained for $K_{d,app}$ (1168 ± 59 μM). The observed agreement indicates that NMT is a nonsticky substrate. Absolute and difference spectra corresponding to 100% conversion of free MTOX to E_{ox}·S (Figure 7, dashed black curves) were calculated using the determined K_d value for the complex, as described in Experimental Procedures.

Slow Phase of the Anaerobic Reaction of Wild-Type MTOX with NMT. The absorption spectrum of EH_2·P exhibits a maximum at 335 nm, as judged by the spectrum observed 62.5 ms after MTOX had been mixed with 2000 μM NMT [$t_{1/2}$(fast phase) = 8.6 ms] (Figure 8A). A 20 nm bathochromic shift of this peak to 355 nm is observed in a slow phase that is complete within 7 s. The slow phase also results in substantial increases in absorption in the near-UV region but virtually no absorbance change is observed above 400 nm (Figure 8A). Absorbance traces at 355 nm exhibit a rapid initial decrease, followed by a slow increase, which can be attributed to the fast and slow phases, respectively, of the reductive half-reaction. Reaction traces at this wavelength give an excellent fit to a double-exponential equation ($y = Ae^{-k_{fast}t} + Be^{-k_{slow}t} + C$) at all substrate concentrations tested (Figure 8A, inset). Values obtained for k_{slow} are independent of the NMT concentration [see Figure 6A (blue circles)] (k_{slow} = 0.981 ± 0.004 s^{-1}). On the other hand, the magnitude of the absorbance change in the near-UV region increases as the concentration of NMT is increased, which can be seen by comparison of reaction traces at 355 nm (Figure 8A, inset) or absorption spectra observed at the end of the slow phase at different NMT concentrations (Figure 8B). The results are consistent with a rate-determining unimolecular dissociation of EH_2·P, followed by a fast bimolecular step to yield an equilibrium mixture of free E and a dead-end reduced enzyme·substrate complex (EH_2·NMT) (Scheme 3, steps 3 and 4). Consistent with this scenario, the final absorbance observed at 355 nm exhibits a hyperbolic dependence on substrate concentration (Figure 8B, inset). The dissociation constant of the complex was estimated by fitting the data to

$$A_{obs} = A_0 + (\Delta A_{max}[NMT])/(K_d + [NMT]) \quad (2)$$

The observed value for the dissociation constant of the EH_2·NMT complex (K_d = 934 ± 218 μM) is very similar to that obtained for the E_{ox}·NMT complex (K_d = 973 ± 42 μM).

The slow phase of the reductive half-reaction is ~100-fold slower than the limiting rate of MTOX reduction in the fast phase or the maximal turnover rate at saturating substrate concentrations (Table 3). The results indicate that the slow phase is not kinetically significant during turnover. This outcome is consistent with the intersecting line double-reciprocal plots obtained in steady-state kinetic studies that indicate that oxygen reacts with EH_2·P.[2]

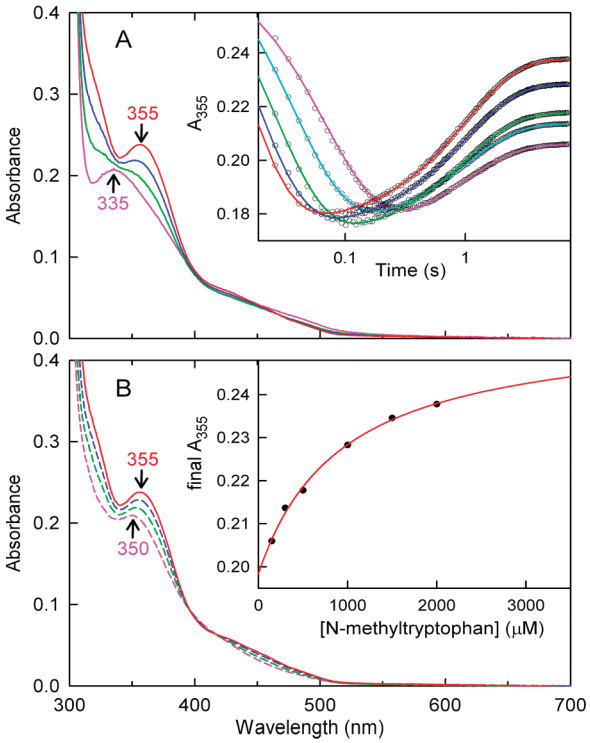

Figure 8. Slow phase of the anaerobic reaction of wild-type MTOX with NMT. Reactions were monitored by stopped-flow diode array spectroscopy. (A) The magenta, green, blue, and red curves were recorded 0.0645, 0.4875, 1.170, and 7.125 s, respectively, after 2000 μM NMT had been mixed with MTOX in 100 mM potassium phosphate buffer (pH 8.0) at 25 °C. In the inset, the magenta, cyan, green, blue, and red curves were obtained by fitting a double-exponential equation ($y = Ae^{-k_{fast}t} + Be^{-k_{slow}t} + C$) to data (●) obtained by monitoring the absorbance change at 355 nm after MTOX had been mixed with 150, 300, 500, 1000, 1500, and 2000 μM NMT, respectively. (B) Final spectra recorded 7.125 s after MTOX had been mixed with 2000, 1000, 500, and 150 μM NMT are shown by the solid red, dashed blue, dashed green, and dashed magenta curves, respectively. The inset shows a plot of the final absorbance at 355 nm observed at 7.125 s vs the concentration of NMT. The solid red line is a fit of a theoretical binding curve [$A_{obs} = A_0 + (\Delta A_{max}[ligand])/(K_d + [ligand])$] to the data (●).

Fast Phase of the Anaerobic Reaction of Lys259Gln with NMT. As detailed below, the fast and slow phases of the reaction with Lys259Gln are less well resolved than those of wild-type MTOX. The best kinetic resolution is achieved with the mutant enzyme at 2000 μM NMT, the highest substrate concentration tested.

An E_{ox}·S complex is formed immediately after the mutant is mixed with 2000 μM NMT, as judged by a bathochromic shift of the 450 nm band of free Lys259Gln to 457 nm (Figure 9A, inset). Unlike wild-type MTOX, negligible conversion of E_{ox}·S to EH_2·P occurs during mixing because of the slower rate of this step with the mutant enzyme (vide infra). The modest spectral perturbation produced upon formation of an E_{ox}·S complex with Lys259Gln is most readily monitored by difference spectroscopy. An isosbestic set of difference spectra are obtained by subtracting

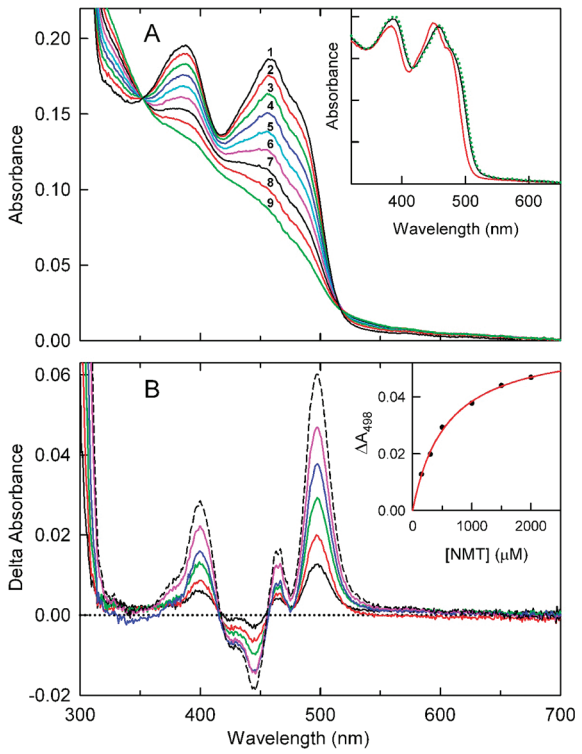

Figure 9. Fast phase of the anaerobic reaction of Lys259Gln with NMT. Reactions were monitored by stopped-flow diode array spectroscopy in 100 mM potassium phosphate buffer (pH 8.0) at 25 °C. (A) Curves 1−9 were recorded 0.00224, 0.0675, 0.1455, 0.2340, 0.3360, 0.4590, 0.6150, 0.8250, and 1.1370 s, respectively, after 14.7 μM enzyme had been mixed with 2000 μM NMT. In the inset, the solid red and solid black curves were recorded 2.24 ms after Lys259Gln had been mixed with 0 and 2000 μM NMT, respectively. The dotted green curve is the spectrum calculated for 100% formation of the enzyme·substrate complex, as described in Experimental Procedures. (B) Difference spectra obtained for formation of the enzyme·substrate complex were generated by subtracting the spectrum of free Lys259Gln from spectra observed 0.74 ms after mixing with various concentrations of NMT. The solid black, red, green, blue, and magenta curves were obtained for reactions with 150, 300, 500, 1000, and 2000 μM NMT, respectively. The dashed black curve shows the difference spectrum calculated for 100% complex formation, as described in Experimental Procedures. The inset shows a plot of the absorbance increase at 498 nm vs NMT concentration. The solid red line is a fit of a theoretical binding curve [$\Delta A_{obs} = (\Delta A_{max}[ligand])/(K_d + [ligand])$] to the data (●).

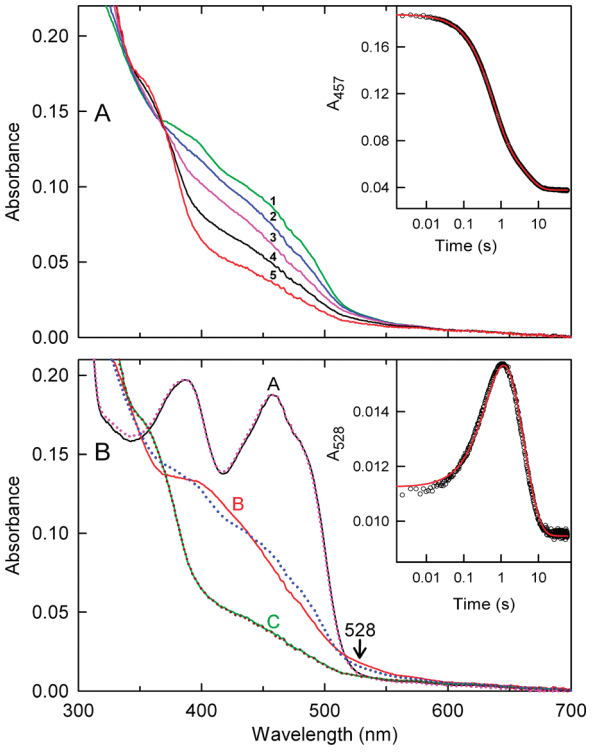

Figure 10. Slow phase (A) and global analysis (B) of the anaerobic reaction of Lys259Gln with NMT. (A) Curves 1−5 were recorded 1.1370, 1.6200, 2.7600, 5.5500, and 59.8500 s, respectively, after the enzyme had been mixed with 2000 μM NMT. In the inset, the red curve was obtained by fitting a double-exponential equation ($y = Ae^{-k_{fast}t} + Be^{-k_{slow}t} + C$) to data (●) obtained by monitoring the reductive half-reaction with 2000 μM NMT at 457 nm. (B) The solid black, red, and green curves show calculated spectra obtained by global fitting of an A ⟹ B ⟹ C model to diode array data obtained for the reaction of Lys259Gln with 2000 μM NMT, as detailed in the text. For comparison, the figure includes spectra observed 0.74 ms (dotted magenta curve), 1.1370 s (dotted blue curve), and 59.8500 s (dotted brown curve) after Lys259Gln had been mixed with 2000 μM NMT. In the inset, the red curve shows the fit of the A ⟹ B ⟹ C model to the observed absorbance change at 528 nm (●).

the spectrum of free Lys259Gln from spectra observed immediately after mixing with different concentrations of NMT. The spectra exhibit a prominent positive peak at 498 nm that can be attributed to the observed bathochromic shift of the 450 nm band of free E_{ox} but provide no evidence of the development of charge-transfer absorption in the long-wavelength region (Figure 9B). A dissociation constant for the mutant E_{ox}·S complex (K_d = 569 ± 69 μM) was obtained by fitting a theoretical binding curve to the observed absorbance increases at 498 nm (Figure 9B, inset). The observed value is 1.7-fold smaller than the K_d obtained for the corresponding wild-type complex (see Table 3). The calculated absolute absorption spectrum for 100% formation of the mutant complex is similar to the initial spectrum observed upon mixing of Lys259Gln with 2000 μM NMT (Figure 9A, inset).

The fast phase of the mutant reaction with 2000 μM NMT exhibits apparent isosbestic points at 352 and 517 nm and is complete within ~1 s (Figure 9A). The fast phase is attributed to the conversion of E_{ox}·NMT to EH_2·P. However, unlike wild-type MTOX, a significant fraction of the total absorbance decrease at 457 nm occurs during the slow phase of the mutant reaction. Consistent with this scenario, the reaction trace obtained at 457 nm with 2000 μM NMT (Figure 10A, inset) or other substrate concentrations gives an excellent fit to a double-exponential equation ($y = Ae^{-k_{fast}t} + Be^{-k_{slow}t} + C$) with just 67.7 ± 0.5% of the absorbance change occurring during the fast phase. Rate constants obtained for the fast phase exhibit a hyperbolic dependence on the concentration of NMT and were fit to eq 1 (Figure 6B). The value obtained for $K_{d,app}$ (424 ± 13 μM) is similar to the K_d value determined for the mutant E_{ox}·NMT complex (Table 3), indicating that NMT is a non-sticky substrate, as observed with wild-type MTOX. The limiting rate of the fast phase (k_{lim} = 2.13 ± 0.02 s^{-1}) is ~60-fold slower than that observed with wild-type MTOX. The results show that the 1300-fold decrease in the apparent turnover rate observed with Lys259Gln cannot be explained by the relatively modest effect of the mutation on the rate of substrate oxidation.

dx.doi.org/10.1021/bi200349m |*Biochemistry* 2011, 50, 4949–4962

Slow Phase of the Anaerobic Reaction of Lys259Gln with NMT. The slow phase of the mutant reaction with 2000 μM NMT occurs from ~1 to 60 s after mixing and exhibits an approximate isosbestic point around 368 nm (Figure 10A). Values for k_{slow} obtained by analysis of the absorbance change at 457 nm are independent of the NMT concentration [see Figure 6B (blue circles)] ($k_{slow} = 0.244 \pm 0.007$ s^{-1}).[a] The slow phase is attributed to the dissociation of the mutant $EH_2 \cdot P$ complex in a step that is just 4-fold slower than that observed with the corresponding wild-type complex (see Scheme 3, step 3, and Table 3). However, it is worth noting that the "slow" step in the reductive half-reaction with Lys259Gln is actually 15-fold faster than the apparent turnover rate of the mutant (see Table 1). The results indicate that oxygen is likely to react with EH_2 during turnover of the mutant enzyme. The same final spectrum is observed for reduced Lys259Gln at all substrate concentrations tested. Thus, unlike the results for wild-type MTOX, the results provide no evidence of the formation of an $EH_2 \cdot$NMT complex with the mutant enzyme.[b]

Global Analysis of the Lys259Gln Reductive Half-Reaction. The true absorption spectrum of $EH_2 \cdot P$ cannot be directly observed with the mutant enzyme because of a relatively modest difference in the rates of the fast and slow phases of the reductive half-reaction, even at a high substrate concentration (e.g., 7.2-fold difference at 2000 μM NMT). To determine the absorption spectrum of $EH_2 \cdot P$, diode array data sets obtained at each NMT concentration were analyzed globally by fitting the data to an A ⟹ B ⟹ C model. In this model, A is an equilibrium mixture of E_{ox} and $E_{ox} \cdot$NMT, B is $EH_2 \cdot P$, and C is EH_2. Rate constants obtained for the fast and slow phases of the reaction by global analysis are very similar to values obtained from single-wavelength analyses (see Table 3). Calculated absorption spectra for A and C at each substrate concentration tested are virtually indistinguishable from the corresponding observed initial and final spectra, respectively, as illustrated in Figure 10B for the reaction with 2000 μM NMT. On the other hand, the calculated spectrum of B, although similar, is clearly not identical to the spectrum observed at the approximate end of the fast phase of the reaction with 2000 μM NMT (Figure 10B). Importantly, the same spectrum is calculated for B at all substrate concentrations tested. The calculated spectrum of B exhibits (i) a broad plateau in the region from 367 and 397 nm and (ii) absorption significantly higher than that of either species A or C above 516 nm, with a maximum increase at 528 nm. Indeed, absorbance traces at 528 nm exhibit a rapid increase, followed by a slow decrease, and give a remarkably good fit to the A ⟹ B ⟹ C model, despite the small amplitude of the observed absorbance change (Figure 10B, inset).

Reaction of Reduced Lys259Gln or Wild-Type MTOX with Oxygen. The kinetics observed for the reductive half-reaction with Lys259Gln strongly suggest that the 1300-fold decrease in the apparent turnover rate of the mutant is due to a large decrease in the rate of reaction of the reduced enzyme with oxygen. Indeed, we found that oxidation of reduced Lys259Gln over a substantial range of oxygen concentrations is slow enough to be monitored in a manual mixing experiment using a steady-state diode array spectrophotometer. An isosbestic conversion of reduced to oxidized mutant enzyme is observed in reactions that exhibit apparent first-order kinetics, as judged by the single-exponential fits obtained at all oxygen concentrations tested (Figure 11A). The observed rate constants are directly proportional to the oxygen concentration (Figure 11B). Strikingly, the second-order rate constant determined for the reaction of reduced Lys259Gln with oxygen ($k = 87 \pm 2$ M^{-1} s^{-1}) is actually 3-fold slower than the very slow reaction observed with free reduced flavin (Table 4). The second-order rate constant obtained for the Lys259Gln reaction was used to calculate an apparent first-order rate constant for the mutant reaction with 273 μM oxygen, the oxygen concentration at which apparent turnover rates are measured. The calculated rate constant ($k = 0.0238 \pm 0.0005$ s^{-1}) is in very good agreement with the observed value of $k_{cat,app}$ with Lys259Gln (0.0166 ± 0.0007 s^{-1}) (see Table 1). The results provide compelling evidence that the 1300-fold decrease in the apparent turnover rate can be entirely attributed to an enormous decrease in the oxygen reactivity of the reduced mutant enzyme.

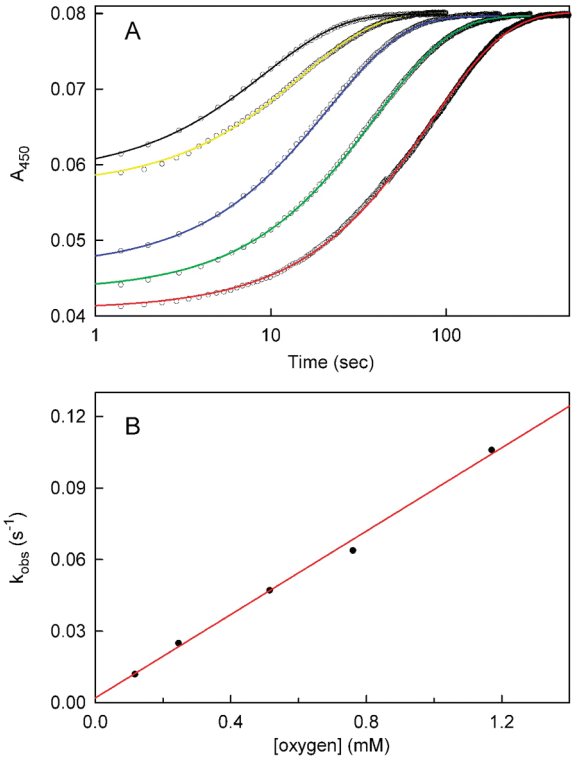

Figure 11. Kinetics of the reaction of reduced Lys259Gln with molecular oxygen. Reactions were conducted with 6.11 μM enzyme in 100 mM potassium phosphate buffer (pH 8.0) at 25 °C. Reaction progress was monitored by steady-state diode array spectroscopy. (A) The red, green, blue, yellow, and black curves were obtained by fitting an equation for a single-exponential rise [$y = A(1 - e^{-kt}) + B$] to data (●) obtained after the reduced enzyme had been mixed with 0.1170, 0.2457, 0.5148, 0.7605, and 1.1700 mM oxygen, respectively. (B) The red line was generated by linear regression analysis of rate constants observed at various oxygen concentrations (●).

Table 4. Rate Constants for the Oxidation of Reduced Wild-Type MTOX or the Lys259Gln Mutant by Molecular Oxygen

preparation	k_{obs} (M^{-1} s^{-1})	$k_{cat}/K_{m,oxygen}$ (M^{-1} s^{-1})[a]
wild-type	$(2.13 \pm 0.07) \times 10^5$	$(1.3 \pm 0.3) \times 10^5$
Lys259Gln	87 ± 2	
free flavin[b]	250	

[a] Data from ref 2. [b] Data from ref 11.

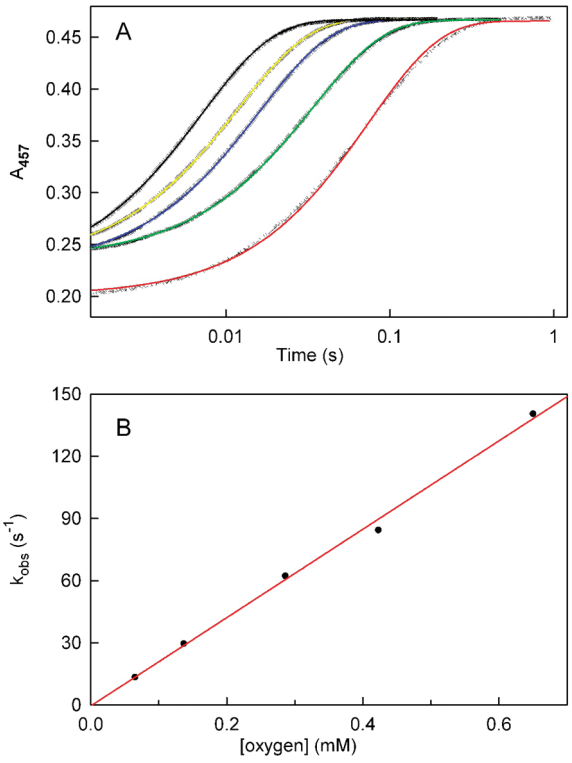

Figure 12. Kinetics of the reaction of reduced wild-type MTOX with molecular oxygen. Reactions were conducted with 35.2 μM enzyme in 100 mM potassium phosphate buffer (pH 8.0) at 25 °C. Reaction progress was monitored at 457 nm using a stopped-flow spectrometer in photomultiplier mode. (A) The red, green, blue, yellow, and black curves were obtained by fitting an equation for a single-exponential rise $[y = A(1 - e^{-kt}) + B]$ to data (●) obtained after the reduced enzyme had been mixed with 0.0650, 0.1365, 0.2860, 0.4225, and 0.6500 mM oxygen, respectively. (B) The red line was generated by linear regression analysis of rate constants observed at various oxygen concentrations (●).

In contrast, reaction of reduced wild-type MTOX with oxygen occurs in an extremely rapid reaction that can be monitored only by using a stopped-flow spectrophotometer in photomultiplier mode. The reaction at all concentrations of oxygen tested exhibits a monoexponential increase in absorption at 457 nm due to the formation of the oxidized enzyme (Figure 12A). The observed rate constants are directly proportional to the oxygen concentration (Figure 12B). Importantly, the second-order rate constant obtained for the oxidation of reduced wild-type MTOX $[k = (2.13 \pm 0.07) \times 10^5\ M^{-1}\ s^{-1}]$ is 2500-fold greater than that of the corresponding reaction with Lys259Gln (Table 4).

DISCUSSION

Mutation of Lys259 in MTOX to a neutral residue (Gln, Ala, or Met) essentially blocks covalent incorporation of FAD during expression of the recombinant proteins in *E. coli*. The small amount of holoenzyme (<5%) in the isolated mutant preparations contains two chromophores: FAD and a modified flavin, identified as 6-hydroxyFAD. Both flavins are covalently bound to the protein and can be reduced by dithionite. However, only FAD is reduced by NMT. The relative amount of 6-hydroxyFAD is affected by the nature of the substitution, increasing in the following order: Lys259Gln < Lys259Ala < Lys259Met. 6-Hydroxyflavins have been found in at least seven other flavoenzymes[19,23−27] (e.g., glycolate oxidase, D-aspartate oxidase, trimethylamine dehydrogenase, and human apoptosis-inducing protein).

The apoprotein in the isolated MTOX mutant preparations can be reconstituted with FAD in reactions that result in the exclusive covalent incorporation of unmodified FAD. The reconstituted preparations exhibit 30−40% of the holoenzyme content observed with wild-type MTOX. The results indicate that Lys259 plays a crucial role in the biosynthesis of the MTOX holoenzyme under physiological conditions. Substitution of Lys259 with a neutral residue does not, however, block in vitro flavinylation of the apoprotein in the isolated mutant preparations. The basis for this difference is unclear. Similar effects on holoenzyme biosynthesis are, however, observed with MSOX when the corresponding lysine (Lys265) is replaced with a neutral residue.[13]

Lys259 is a catalytically important residue in MTOX, as judged by the huge decrease in the apparent turnover rate observed with the reconstituted mutant preparations. Reductive and oxidation half-reaction studies with reconstituted Lys259Gln show that the 1300-fold decrease in the apparent turnover rate is entirely due to an enormous decrease (2500-fold) in the oxygen reactivity of the reduced enzyme. Indeed, reaction of reduced Lys259Gln with oxygen is 3-fold slower than the already sluggish reaction observed with free reduced FAD. The results provide compelling evidence that Lys259 is the site of oxygen activation in MTOX.

It is noteworthy that covalently bound reduced FAD not only is produced as a catalytic intermediate during aerobic turnover of MTOX but also is formed as the penultimate species in the pathway for the biosynthesis of the covalent flavin linkage.[20] Thus, it is perhaps not surprising that mutation of Lys259 might affect both catalysis and holoenzyme biosynthesis. Interestingly, studies with trimethylamine dehydrogenase and human apoptosis-inducing protein show that (i) 6-hydroxyflavin is produced during the oxidation of the reduced enzymes and (ii) the 6-hydroxyl group is derived from molecular oxygen.[25−27] The results suggest that incorporation of 6-hydroxyFAD into the MTOX mutants may result from an aberrant reaction of oxygen with reduced mutant enzyme, produced in vivo during flavinylation of the apoenzyme or turnover of the holoenzyme with endogenous NMT.

Lys259 is located just above the *si* face of the flavin ring in MTOX, whereas the binding site for NMT is above the *re* face of the flavin ring.[5] The results show that MTOX contains two physically distinct active sites for oxygen reduction and substrate oxidation, as observed with MSOX[13] and postulated for several other oxidases.[28−30] Although located on the opposite side of the flavin ring, Lys259 also exerts a strong, presumably electrostatic, influence on the microenvironment at the active site for NMT oxidation, as discussed below.

Mutation of Lys259 Alters the Composition and Reactivity of the Oxidized Enzyme·Substrate Complex (E_{ox}·NMT). Wild-type MTOX forms an E_{ox}·NMT complex at pH 8.0 that exhibits significant absorption in the long-wavelength region (λ > 550 nm) that can be attributed to charge-transfer interaction. In this complex, oxidized FAD and NMT act as the charge-transfer acceptor and donor, respectively. Charge-transfer interaction with NMT as the donor is possible only with the electron-rich anionic form of NMT [R-CH-(CO_2^-)-NH-CH_3]. The amino acid anion is also the redox-active form that is oxidized in the second step of the catalytic cycle (see Scheme 3, step 2).[1,31] The

zwitterionic form of NMT is, however, the major species in solution at pH 8.0 ($pK_a \sim 10$). The results indicate that the pK_a of NMT bound to wild-type MTOX must be considerably below the pK_a of the free amino acid. In contrast, the mutant E_{ox}·NMT complex exhibits no evidence of charge-transfer interaction at pH 8.0.[c] The results strongly suggest that the positive charge of Lys259 plays a major role in the selective stabilization of an oxidized enzyme complex with the reactive amino acid anion. Consistent with this hypothesis, conversion of the mutant E_{ox}·NMT complex to a reduced enzyme·imine product complex (EH_2·P) is 60-fold slower than the corresponding reaction with wild-type enzyme. Replacement of Lys259 with a neutral residue may also lower the flavin redox potential, a factor that could contribute to the observed decrease in the rate of NMT oxidation.

Mutation of Lys259 Affects the Properties and Catalytic Role of the Reduced Enzyme·Imine Product Complex (EH_2·P). The wild-type EH_2·P complex exhibits a typical reduced flavin spectrum (λ_{max} = 335 nm) with very low absorbance in the 450 nm region. In contrast, the mutant complex exhibits a broad plateau centered around 380 nm, and substantial absorbance at longer wavelengths. Indeed, conversion of the mutant E_{ox}·NMT complex to the EH_2·P complex is accompanied by a transient increase in absorbance at 528 nm (see Figure 10B, inset). The observed spectral properties of the mutant EH_2·P complex are attributed to charge-transfer interaction between reduced FAD and the positively charged iminium moiety in the zwitterionic oxidation product [R-CH-(CO_2^-)-NH^+=CH_2]. In contrast, the wild-type EH_2·P complex exhibits no evidence of charge-transfer interaction and is likely to contain the anionic form of the imine product [R-CH-(CO_2^-)-N=CH_2], a species that cannot act as a charge-transfer acceptor. Thus, a simple difference in ligand protonation state, zwitterionic or anionic, can account for the different properties observed for both E_{ox}·NMT and EH_2·P complexes formed with mutant or wild-type MTOX, respectively. The charge-transfer EH_2·P complex observed with the Lys259Gln MTOX mutant exhibits spectral properties similar to those of analogous complexes formed with (i) MSOX when the corresponding lysine (Lys265) is replaced with a neutral residue[13] and (ii) wild-type dimethylglycine oxidase.[32]

Dissociation of the EH_2·P complex formed with wild-type MTOX is ~100-fold slower than k_{cat} and therefore not kinetically significant during turnover. This outcome and the intersecting line double-reciprocal plots obtained in steady-state kinetic studies[2] indicate that the EH_2·P complex is the species that reacts with oxygen during turnover of wild-type MTOX. Free reduced enzyme (EH_2) is produced upon incubation of wild-type MTOX with 1 equiv of NMT for 30 min to ensure complete reduction prior to use in oxidative half-reaction studies. The steady-state kinetic parameter, $k_{cat}/K_{m,oxygen}$, provides an approximate estimate of the rate of reaction of oxygen with EH_2·P. The value obtained for $k_{cat}/K_{m,oxygen}$ with wild-type MTOX [$(1.3 \pm 0.3) \times 10^5$ M^{-1} s^{-1}][2] is similar to the second-order rate constant observed for the oxidation of EH_2 in stopped-flow studies [$k = (2.13 \pm 0.07) \times 10^5$ M^{-1} s^{-1}]. The results indicate that (i) the reactivity of the reduced wild-type enzyme with oxygen is not apparently affected by the presence of bound product and (ii) EH_2 is not a catalytically competent intermediate, despite its high reactivity with oxygen, because dissociation of EH_2·P is much slower than the reaction of the complex with oxygen. In contrast, dissociation of the mutant EH_2·P complex, although 4-fold slower than that observed for the wild-type complex, is 15-fold faster than the apparent turnover rate of the mutant. Thus, free EH_2 is the species that reacts with oxygen during turnover of the mutant enzyme in air-saturated buffer because dissociation of the EH_2·P complex is faster than its very sluggish reaction with oxygen.

Concluding Remarks. The pleiotropic effects observed upon mutation of Lys259 reveal its multiple functions in MTOX biosynthesis and catalysis and especially highlight the critical role of the residue in the activation of molecular oxygen. The results provide definitive evidence for Lys259 being the site of oxygen activation in MTOX and show that a single basic amino acid residue is entirely responsible for the enormous rate acceleration observed with the wild-type enzyme. The two-electron reduction of oxygen by reduced flavin proceeds via an initial one-electron-transfer step that generates a flavin radical/superoxide anion radical pair in a spin-allowed but energetically unfavorable, rate-determining reaction[11,12] (see Scheme 1). The reorganization energy required to change the configuration of the surrounding medium constitutes the major energy barrier in the one-electron reduction of oxygen.[33] We propose that Lys259 accelerates the reaction of reduced MTOX with oxygen by providing a preorganized binding site for the superoxide anion intermediate.[d] The results obtained with MTOX and in previous studies with MSOX[13,14] strongly suggest that the corresponding lysine will be the site of oxygen activation in other members of the MTOX−MSOX family (e.g., pipecolate oxidase, fructosyl amino acid oxidase[8,9]). Consequently, these oxidases are also expected to contain separate active sites for oxygen reduction and amino acid oxidation on opposite faces of the flavin ring, as observed with MTOX and MSOX.

A lysine residue hydrogen bonded to flavin N5 via a bridging water appears to be a common motif in other flavoprotein oxidases, as judged by structures observed for monoamine oxidase B,[34] polyamine oxidase,[35] monoamine oxidase A,[36] L-amino acid oxidase,[37] and LSD1, a lysine-specific histone demethylase.[38] There is only limited information available regarding the role of these active site lysine residues. However, it has been shown that catalytic activity is abolished upon mutation of Lys296 in monoamine oxidase B or Lys661 in LSD1.[39,40] Recent molecular dynamic simulations of the diffusion of oxygen into LSD1 suggest that Lys661 may play a role in oxygen activation by this enzyme.[29] On the other hand, Lys300 in maize polyamine oxidase plays a major role in substrate oxidation, as judged by a 1400-fold decrease in the limiting rate of flavin reduction observed with a Lys300Met mutant.[41] In sharp contrast, the equivalent mutation in mouse polyamine oxidase (Lys315Met) does not affect the rate of flavin reduction.[42] However, the lysine mutations in both maize and mouse polyamine oxidase cause a similar, albeit modest, decrease (30- and 25-fold, respectively) in the oxygen reactivity of the reduced enzymes.[42,43] Surprisingly, the reaction with oxygen is faster when the lysine is uncharged, as judged by studies with mouse polyamine oxidase.[42] The results indicate that, unlike MTOX or MSOX, the active site lysine in maize and mouse polyamine oxidase plays a relatively minor, nonelectrostatic role in oxygen activation.

In summary, the Lys NZ−Wat−FAD N5 motif can exhibit an impressive range of functions within a single enzyme and also considerable functional diversity among homologous enzymes, as illustrated by results obtained with MTOX and the polyamine oxidases, respectively. The motif is found in nearly all members of the MTOX−MSOX family of amino acid oxidases where it is

likely to emerge as the principal factor responsible for oxygen activation. However, other unknown elements must be in place to support this functionality, as judged by the fact that it is not absolutely conserved in other oxidases that also harbor the motif. The results indicate that oxygen activation by flavo-oxidases is mechanistically complex and not fully understood.

■ ASSOCIATED CONTENT

Supporting Information. Primers used for mutagenesis (Table S1) and properties of His_6-tagged wild-type MTOX (Table S2). This material is available free of charge via the Internet at http://pubs.acs.org.

■ AUTHOR INFORMATION

Corresponding Author

*Phone: (215) 762-7495. Fax: (215) 762-4452. E-mail: marilyn.jorns@drexelmed.edu.

Notes

[a]Similar values for k_{slow} are obtained upon analysis of the biphasic absorbance change at 355 nm (see Table 3).

[b]It is, however, possible that formation of an EH_2·NMT complex does occur with Lys259Gln but cannot be detected because the complex and free EH_2 exhibit similar spectral properties.

[c]A similar absorption spectrum is observed at pH 9.4 for a complex of wild-type MTOX with sarcosine, a poor substrate.[1] The limiting rate of sarcosine reduction of wild-type MTOX is comparable to that observed with Lys259Gln and NMT. However, binding of sarcosine to wild-type MTOX is 400-fold weaker than binding of NMT to Lys259Gln. MTOX-bound sarcosine exhibits a pK_a of 9.1.[1] The inability of the poor substrate to form a charge-transfer complex with wild-type MTOX at pH 9.4 suggests that the ligand is not properly positioned for charge-transfer interaction with FAD, an apparent prerequisite for rapid substrate oxidation.

[d]Lys259 may also play a secondary role in subsequent proton-transfer steps, either from N5 of reduced FAD or to superoxide or peroxide intermediates.

Funding Sources

This work was supported in part by Grant GM 31704 (M.S.J.) from the National Institutes of Health.

■ ABBREVIATIONS

MTOX, *N*-methyltryptophan oxidase; NMT, *N*-methyl-L-tryptophan; MSOX, monomeric sarcosine oxidase; FAD, flavin adenine dinucleotide; PDB, Protein Data Bank.

■ REFERENCES

(1) Ralph, E. C., and Fitzpatrick, P. F. (2005) pH and kinetic isotope effects on sarcosine oxidation by N-methyltryptophan oxidase. *Biochemistry 44*, 3074–3081.

(2) Khanna, P., and Jorns, M. S. (2001) N-Methyltryptophan oxidase from *Escherichia coli*: Reaction kinetics with N-methyl amino acid and carbinolamine substrates. *Biochemistry 40*, 1451–1459.

(3) Khanna, P., and Jorns, M. S. (2001) Characterization of the FAD-containing N-methyltryptophan oxidase from *Escherichia coli*. *Biochemistry 40*, 1441–1450.

(4) Wagner, M. A., Khanna, P., and Jorns, M. S. (1999) Structure of the flavocoenzyme of two homologous amine oxidases: Monomeric sarcosine oxidase and N-methyltryptophan oxidase. *Biochemistry 38*, 5588–5595.

(5) Ilari, A., Bonamore, A., Franceschini, S., Fiorillo, A., Boffi, A., and Colotti, G. (2008) The X-ray structure of N-methyltryptophan oxidase reveals the structural determinants of substrate specificity. *Proteins 71*, 2065–2075.

(6) Trickey, P., Wagner, M. A., Jorns, M. S., and Mathews, F. S. (1999) Monomeric sarcosine oxidase: Structure of a covalently-flavinylated secondary amine oxidizing enzyme. *Structure 7*, 331–345.

(7) Carrell, C. J., Bruckner, R. C., Venci, D., Zhao, G., Jorns, M. S., and Mathews, F. S. (2007) NikD, an unusual amino acid oxidase essential for nikkomycin biosynthesis: Structures of closed and open forms at 1.15 and 1.90 Å resolution. *Structure 15*, 928–941.

(8) Dodt, G., Kim, D. G., Reimann, S. A., Reuber, B. E., McCabe, K., Gould, S. J., and Mihalik, S. J. (2000) L-Pipecolic acid oxidase, a human enzyme essential for the degradation of L-pipecolic acid, is most similar to the monomeric sarcosine oxidases. *Biochem. J. 345*, 487–494.

(9) Collard, F., Zhang, J., Nemet, I., Qanungo, K. R., and Monnier, V. M. (2008) Crystal structure of the deglycating enzyme fructosamine oxidase (amadoriase II). *J. Biol. Chem. 283*, 27007–27016.

(10) Kvalnes-Krick, K., and Jorns, M. S. (1991) Role of the covalent and noncovalent flavins in sarcosine oxidase. In *Chemistry and Biochemistry of Flavoenzymes* (Muller, F., Ed.) pp 425−435, CRC Press Inc., Boca Raton, FL.

(11) Massey, V. (1994) Activation of molecular oxygen by flavins and flavoproteins. *J. Biol. Chem. 269*, 22459–22462.

(12) Klinman, J. P. (2007) How do enzymes activate oxygen without inactivating themselves? *Acc. Chem. Res. 40*, 325–333.

(13) Zhao, G., Bruckner, R. C., and Jorns, M. S. (2008) Identification of the oxygen activation site in monomeric sarcosine oxidase: Role of Lys265 in catalysis. *Biochemistry 47*, 9124–9135.

(14) Jorns, M. S., Chen, Z., and Mathews, F. S. (2010) Structural characterization of mutations at the oxygen activation site in monomeric sarcosine oxidase. *Biochemistry 49*, 3631–3639.

(15) Kommoju, P. R., Bruckner, R. C., Ferreira, P., Carrell, C. J., Mathews, F. S., and Jorns, M. S. (2009) Factors that affect oxygen activation and coupling of the two redox cycles in the aromatization reaction catalyzed by nikD, an unusual amino acid oxidase. *Biochemistry 48*, 9542–9555.

(16) Ghanem, M., and Gadda, G. (2005) On the catalytic role of the conserved active site residue His466 of choline oxidase. *Biochemistry 44*, 893–904.

(17) Gadda, G., Fan, F., and Hoang, J. V. (2006) On the contribution of the positively charged headgroup of choline to substrate binding and catalysis in the reaction catalyzed by choline oxidase. *Arch. Biochem. Biophys. 451*, 182–187.

(18) Ho, S. N., Hunt, H. D., Horton, R. M., Pullen, J. K., and Pease, L. R. (1989) Site-directed mutagenesis by overlap extension using the polymerase chain reaction. *Gene 77*, 51–59.

(19) Mayhew, S. G., Whitfield, C. D., Ghisla, S., and Jorns, M. S. (1974) Identification and properties of new flavins in electron-transferring flavoprotein from *Peptostreptococcus elsdenii* and pig liver glycolic acid oxidase. *Eur. J. Biochem. 44*, 579–591.

(20) Hassan-Abdallah, A., Bruckner, R. C., Zhao, G., and Jorns, M. S. (2005) Biosynthesis of covalently bound flavin: Isolation and in vitro flavinylation of the monomeric sarcosine oxidase apoprotein. *Biochemistry 44*, 6452–6462.

(21) Bruckner, R. C., and Jorns, M. S. (2009) Spectral and kinetic characterization of intermediates in the aromatization reaction catalyzed by nikD, an unusual amino acid oxidase. *Biochemistry 48*, 4455–4465.

(22) Zhao, G., and Jorns, M. S. (2006) Spectral and kinetic characterization of the Michaelis charge transfer complex in monomeric sarcosine oxidase. *Biochemistry 45*, 5985–5992.

(23) Negri, A., Massey, V., and Williams, C. H. J. (1987) D-Aspartate oxidase from beef kidney. *J. Biol. Chem. 262*, 10026–10034.

(24) Igarashi, K., Verhagen, M. F. J. M., Samejima, M., Schulein, M., Eriksson, K. L., and Nishino, T. (1999) Cellobiose dehydrogenase from the fungi *Phanerochaete chrysosporium* and *Humicola insolens*. *J. Biol. Chem. 274*, 3338–3344.

(25) Marshall, K. R., Gong, M., Wodke, L., Lamb, J. H., Jones, D. J. L., Farmer, P. B., Scrutton, N. S., and Munro, A. W. (2005) The human apoptosis-inducing protein AMID is an oxidoreductase with a modified flavin cofactor and DNA binding activity. *J. Biol. Chem. 280*, 30735–30740.

(26) Huang, L. X., Scrutton, N. S., and Hille, R. (1996) Reaction of the C30A mutant of trimethylamine dehydrogenase with diethylmethylamine. *J. Biol. Chem. 271*, 13401–13406.

(27) Lu, X. L., Nikolic, D., Mitchell, D. J., van Breemen, R. B., Mersfelder, J. A., Hille, R., and Silverman, R. B. (2003) A mechanism for substrate-induced formation of 6-hydroxyflavin mononucleotide catalyzed by C30A trimethylamine dehydrogenase. *Bioorg. Med. Chem. Lett. 13*, 4129–4132.

(28) Forneris, F., Heuts, D. P. H. M., Delvecchio, M., Rovida, S., Fraaije, M. W., and Mattevi, A. (2008) Structural analysis of the catalytic mechanism and stereo selectivity in *Streptomyces coelicolor* alditol oxidase. *Biochemistry 47*, 978–985.

(29) Baron, R., Binda, C., Tortorici, M., McCammon, J. A., and Mattevi, A. (2011) Molecular mimicry and ligand recognition in binding and catalysis by the histone demethylase LSD1-CoREST complex. *Structure 19*, 212–220.

(30) Saam, J., Rosini, E., Molla, G., Schulten, K., Pollegioni, L., and Ghisla, S. (2010) O_2 reactivity of flavoproteins: Dynamic access of dioxgen to the active site and role of a H^+ relay system in D-amino acid oxidase. *J. Biol. Chem. 285*, 24439–24446.

(31) Zhao, G., and Jorns, M. S. (2002) Monomeric sarcosine oxidase: Evidence for an ionizable group in the ES complex. *Biochemistry 41*, 9747–9750.

(32) Basran, J., Bhanji, N., Basran, A., Nietlispach, D., Mistry, S., Meskys, R., and Scrutton, N. S. (2002) Mechanistic aspects of the covalent flavoprotein dimethylglycine oxidase of *Arthrobacter globiformis* studied by stopped-flow spectrophotometry. *Biochemistry 41*, 4733–4743.

(33) Lind, J., Shen, X., Merenyi, G., and Jonsson, B. O. (1989) Determination of the rate constant of self-exchange of the $O_2/O_2^{\bullet-}$ couple in water by $^{18}O/^{16}O$ isotope marking. *J. Am. Chem. Soc. 111*, 7654–7655.

(34) Binda, C., Li, M., Hubalek, F., Restelli, N., Edmondson, D. E., and Mattevi, A. (2003) Insights into the mode of inhibition of human mitochondrial monoamine oxidase B from high-resolution crystal structures. *Proc. Natl. Acad. Sci. U.S.A. 100*, 9750–9755.

(35) Binda, C., Coda, A., Angelini, R., Federico, R., Ascenzi, P., and Mattevi, A. (1999) A 30 angstrom long U-shaped catalytic tunnel in the crystal structure of polyamine oxidase. *Structure 7*, 265–276.

(36) Son, S., Ma, J., Kondou, Y., Yoshimura, M., Yamashita, E., and Tsukihara, T. (2008) Structure of human monoamine oxidase A at 2.2 Å resolution: The control of opening the entry for substrates/inhibitors. *Proc. Natl. Acad. Sci. U.S.A. 105*, 5739–5744.

(37) Pawelek, P. D., Cheah, J., Coulombe, R., Macheroux, P., Ghisla, S., and Vrielink, A. (2000) The structure of L-amino acid oxidase reveals the substrate trajectory into an enantiomerically conserved active site. *EMBO J. 19*, 4204–4215.

(38) Chen, Y., Yang, Y., Wang, F., Wan, K., Yamane, K., Zhang, Y., and Lei, M. (2006) Crystal structure of human histone lysine-specific demethylase 1 (LSD1). *Proc. Natl. Acad. Sci. U.S.A. 103*, 13956–13961.

(39) Kacar, B., and Edmondson, D. E. (2006) Studies on the role of lysine-296 in human mitochondrial monoamine oxidase B catalysis. *FASEB J. 20*, A478–A479.

(40) Lee, M. G., Wynder, C., Cooch, N., and Shiekhattar, R. (2005) An essential role for CoREST in nucleosomal histone 3 lysine 4 demethylation. *Nature 437*, 432–435.

(41) Polticelli, F., Basran, J., Faso, C., Cona, A., Minervini, G., Angelini, R., Federico, R., Scrutton, N. S., and Tavladoraki, P. (2005) Lys300 plays a major role in the catalytic mechanism of maize polyamine oxidase. *Biochemistry 44*, 16108–16120.

(42) Pozzi, M. H., and Fitzpatrick, P. F. (2010) A lysine conserved in the monoamine oxidase family is involved in oxidation of the reduced flavin in mouse polyamine oxidase. *Arch. Biochem. Biophys. 498*, 83–88.

(43) Fiorillo, A., Federico, R., Polticelli, F., Boffi, A., Mazzei, F., Di Fusco, M., Ilari, A., and Tavladoraki, P. (2011) The structure of maize polyamine oxidase K300M mutant in complex with the natural substrates provides a snapshot of the catalytic mechanism of polyamine oxidation. *FEBS J. 278*, 809–821.